



Structure impact of two galactomannan fractions on their viscosity properties in dilute solution, unperturbed state and gel state

Sébastien Gillet, Mario Aguedo, Raul Petrut, Gilles Olive, Paul Anastas, Christophe Blecker, Aurore Richel

► To cite this version:

Sébastien Gillet, Mario Aguedo, Raul Petrut, Gilles Olive, Paul Anastas, et al.. Structure impact of two galactomannan fractions on their viscosity properties in dilute solution, unperturbed state and gel state. *International Journal of Biological Macromolecules*, 2017, 96 (3), pp.550-559. 10.1016/j.ijbiomac.2016.12.057 . hal-01429483

HAL Id: hal-01429483

<https://hal.science/hal-01429483>

Submitted on 12 Jan 2017

HAL is a multi-disciplinary open access archive for the deposit and dissemination of scientific research documents, whether they are published or not. The documents may come from teaching and research institutions in France or abroad, or from public or private research centers.

L'archive ouverte pluridisciplinaire **HAL**, est destinée au dépôt et à la diffusion de documents scientifiques de niveau recherche, publiés ou non, émanant des établissements d'enseignement et de recherche français ou étrangers, des laboratoires publics ou privés.

***Structure impact of two galactomannan fractions on their viscosity properties
in dilute solution, unperturbed state and gel state***

GILLET SÉBASTIEN^{*ab}. Tel. : +32.81622230. Email : s.gillet@yale.edu

AGUEDO MARIO^a mario.aguedo@ulg.ac.be

PETRUTRAUL^c rfpetrut@student.ulg.ac.be

OLIVE GILLES^{ac} gilles.olive@ulg.ac.be

ANASTAS PAUL^b paul.anastas@yale.edu

BLECKER CHRISTOPHE^c christophe.blecker@ulg.ac.be

RICHEL AURORE^a a.richel@ulg.ac.be

* Corresponding author

^a University of Liège – Gembloux Agro-Bio Tech, Unit of Biological and Industrial Chemistry (CBI).
2, Passage des déportés , 5030 Gembloux. Belgium.

^b Yale University – Center for Green Chemistry and Green Engineering .
370 Prospect Street, Greeley Memorial Lab 2A, New Haven CT 06511. USA.

^c University of Liège – Gembloux Agro-Bio Tech, Food Science and Formulation Department (SAF).
2, Passage des déportés, 5030 Gembloux. Belgium.

This research did not receive any specific grant from funding agencies in the public, commercial, or not-for-profit sectors.

1. Introduction

Locust bean gum (LBG) is a food additive (E410) used mainly in the industry for its rheological, texturing and gelling properties[1]. LBG is made from the endosperm of the seeds of the carob tree (*Ceratonia siliqua* L.). The endosperm is composed of reserve polysaccharides (hemicelluloses) called galactomannans. Galactomannans consist of a β -(1 \rightarrow 4)-D-mannopyranosyl backbone substituted to varying degrees at α -(1 \rightarrow 6) with single D-galactopyranosyl residues [2]. The basic structure is the same for all galactomannans. Three elements, however, allow distinction between these polysaccharides: (i) the degree of galactose substitution (DS_{Gal}), (ii) the molecular weights, and (iii) the distribution pattern of galactosyl substituents along the main chain of mannans [3]. The fine structure of galactomannans of locust bean is most likely composed of "smooth" zones (lowly substituted) and "hairy" zones, i.e. much denser in side-galactosyls, without being systematically adjacent [4]. In the industrial production process of LBG [5], the purification step has a major influence on the composition and properties of gums. During clarification, the dissolution temperature is a crucial parameter which influences the average chemical structure of the resulting gum, also correlated to the viscosity observed in aqueous solution or dispersion [1]. In dilute solutions, the intrinsic viscosity is influenced by the fine chemical structure of galactomannans [4], itself defining the conformation of the polymer coil. The degree of space occupancy of a coil present in a polymer solution at a given concentration (C) may be characterized by the dimensionless "coil overlap parameter" $C[\eta]$ [6]. Double logarithmic plots of specific viscosity (η_{sp}) versus $C[\eta]$ for a range of random coil polysaccharides were found to closely superimpose over one another, and fall into two linear regions, with an abrupt change in slope, when critical concentration C^* is reached. C^* depends on the hydrodynamic volume and corresponds to the transition from dilute to semi-dilute solutions, when concentration increases. It appears that the volume occupied by the isolated polymer coils decreases with concentration. At concentrations greater than C^* , the polymer coils compress. This compression continues until the polymer chains have reached their limiting size at C^{**} , providing a regime called unperturbed state [7]. At $C > C^{**}$ the limited size coils have to interpenetrate more and more [8]. The existence of this second transition at C^{**} , which marks the onset of the concentrated regime, was predicted from scaling arguments by de Gennes [9]. The magnitude of these two

transitions will therefore depend upon solvent quality as well as hydrodynamic volume, with more chains increasing the breadth of the semi-dilute region [10]. The distinction between C^* and C^{**} is however not always visible graphically [11] and the transition between the dilute and the concentrated regimes is then generally designated by C^* . Thus in concentrated regime, an increasing concentration in polymers promotes the overlapping of the macromolecular chains and the appearance of entanglement [12]. In these concentrated states other approaches are needed to study the behavior of polymers such as the dynamic viscosity or the viscoelasticity. A viscous solution of LBG can finally generate a gel state when the polymer concentration in the concentrated regime increases or when a contracted hydrogel is formed after the solution was subjected to several freeze-thaw cycles [13, 14, 15].

The present study aims to establish links between the structural differences of two fractionated carob galactomannans samples (99.9 % pure), previously fully characterized, and their viscosity properties over a wide range of polymer concentrations, under: (i) dilute solutions; (ii) unperturbed state; (iii) gel state. The objective is to assess the impact of small structural differences on the physical behavior of these macromolecules and thus to improve the global knowledge about the macromolecular phenomena that determine coil polymer viscosity, as well as the structure-function relationship of galactomannans and their potential industrial applications.

2. Materials and Methods

2.1. Materials

Crude locust bean gum (CLBG) was obtained from PFW Ltd. (Greenford, UK) as the product sold under the trade mark name HERCOGUM N1. All others chemicals were purchased from commercial suppliers and used as received. A purified hot extract (GM80) and a purified cold extract (GM25) were obtained respectively from 80 °C and 25 °C subtractive fractionation treatment of the CLBG sample. Fractionation, analyses of composition and structures determination have been carried out for and as describe in our previous study [4], resulting in two fully-characterized-fractions that were used as starting material in the present study.

2.2. Viscosity and physical properties in solution/dispersion

Three main physical properties of galactomannans in solution/dispersion, which are of interest for industrial potential applications, were investigated.

2.2.1. Intrinsic viscosity and coil overlap parameter.

The specific viscosity (η_{sp}) of a polymer is a dimensionless characteristic: $\eta_{sp} = (\eta_o - \eta_s)/\eta_s$ (Eq. 1), where η_s is the viscosity of the solvent in the absence of polymer and η_o is the viscosity of the solution containing a given concentration of dissolved polymer. The intrinsic viscosity $[\eta]$ (mL/g) is defined as follows: $[\eta] = \lim_{c \rightarrow 0}(\eta_{sp}/C)$ (Eq. 2). To determine $[\eta]$, dilute solutions (0.01 –0.50 g/100 mL) of LBG were prepared by mixing the appropriate amount of GM25 and GM80 fractions in distilled water at 90 °C, under mechanical stirring for 3 h and cooled to room temperature before measurements at 25°C. Specific viscosities (η_{sp}) were measured with a Desreux-Bischoff capillary viscosimeter. The Huggins equation was applicable and was used to calculate the intrinsic viscosities $[\eta]$: $\eta_{sp}/C = [\eta] + \lambda_H[\eta]^2C$ (Eq.3.), where C is the concentration and λ_H the Huggins constant. Another relation, the Kraemer equation, based on the relative viscosity (η_r), in dilute solutions where the specific viscosity is much less than 1, may be constructed: $\ln(\eta_r)/C = [\eta] + \lambda_K[\eta]^2C$ (Eq. 4), where λ_K is the Kraemer constant. A plot of the inherent viscosity, extrapolated to zero concentration, yields the intrinsic viscosity $[\eta]$. Values of intrinsic viscosity were used to construct a double-logarithmic plot of specific viscosity versus $C[\eta]$ to determine the transition at the critical concentration (C^*) between the dilute and the concentrated regimes - which is characteristic of many polymer solutions – and the scaling laws obtained by the slopes of the regression lines of semi-dilute and dilute solution.

2.2.2. Viscosity and viscoelasticity

Rheological properties of carob gum were characterized at 25 °C on carob gum dispersions prepared as follows: 0.5%, 1% and 2% on a dry weight basis in distilled water, 1M NaOH or 1M NaCl at 90 °C, under mechanical stirring for 3 h and cooled to room temperature before measurements. Rheological measurements were performed using a rheometer MCR 302 (Anton Paar, Graz, Austria) equipped

with a temperature control system and with a cone and plate geometry (0.996° cone angle, 49.975 mm plate diameter, 102 μm gap). Each sample (approximately 3 mL) was placed in the sensor system for measurement at 25 °C. The dynamic viscosity η (Pa.s) of semi-dilute solutions is defined as followed $\eta = \sigma/\dot{\gamma}$ (Eq. 5) with σ the shear stress (Pa) and $\dot{\gamma}$ the shear rate (s^{-1}). Dynamic viscosity curves were obtained with the following program: from 0.1 to 1000 s^{-1} with 5 points measured per decade (Log). Zero-shear viscosity (η_0) and shear rate at which viscosity is reduced to $\eta_0/2$ ($\dot{\gamma}_{1/2}$) are obtained from the equation of Morris [16]: $\eta = \eta_0 / [1 + (\dot{\gamma}/\dot{\gamma}_{1/2})]^{0.76}$ (Eq. 6). Oscillatory tests were performed at 25 °C using the same equipment. Variations in G' (storage modulus – elastic component), G'' (loss modulus – viscous component) and η^* (complex viscosity) were recorded as a function of frequency, thus obtaining the characteristic mechanical spectra. Frequency sweeps from 0.1 to 30 Hz were performed at constant strain within the linear viscoelastic range ($\gamma = 0.5\%$). All the measurements were performed at least in duplicate. Brookfield silicone oils respectively 9.2, 95.5 and 4950 cp were used as Newtonian behavior references. Hyperentanglement highlighting was characterized by preparing solutions of galactomannans in alkali (1M NaOH) and comparing their viscosity before and after neutralization with HCl. Experimentally, the volume changes during neutralization were measured, and the polysaccharide concentration in the alkali solution was adjusted to the same value by addition of the appropriate volume of 1M NaOH. Comparison was also made with the same concentration of galactomannan dissolved directly in 1M NaCl.

2.2.3. Analysis of hydrogels with the texture analyzer

Dilute solutions (0.05 – 2 g/100 mL) of LBG were prepared by mixing the appropriate amount of GM25 and GM80 fractions in distilled water at 90 °C, under mechanical stirring for 3 h and cooled to room temperature before three freeze-thaw cycles (-20 °C). If present, the excess water released during the operation was removed before measurements at 25 °C. A sample with a height of 10 mm was placed in a cylindrical vessel in stainless steel (40 mm inner diameter). Gelled samples were prepared by wire-cutting standard-sized cylinder shape (fitted to the vessel) while viscous samples and water were simply poured into the vessel to the desired height. Samples were analyzed with a TA-XT2 texture analyzer (Stable Micro-Systems, Haslemere, UK). Instrumental texture profile analysis (TPA)

methodology consists of compressing the gel sample twice in a reciprocal motion. TPA was performed by means of a 15 mm diameter flat circular probe, penetrating twice for 5 s into the gel at a speed of 60 mm/min (penetration depth = 5 mm). Hardness is defined as the peak force during the first compression cycle; cohesiveness is defined as the ratio of positive force area during the second compression portion to that during the first compression; and springiness is defined as the height that the sample recovered during the time elapsed between the end of the first bite and the start of the second bite [17]. All were averaged using 3 replicate determinations.

3. Results & discussions

3.1. Structural characterization

The fractionation process generated two pure galactomannans fractions (> 99.9 %) with different chemical structures, for which a schematized representation is proposed in Fig. 1. The GM25 fraction consisted of galactomannans composed of shorter chains, richer in galactosyl, which were distributed at 70 % inside “block” structures (grouped in “hairy” regions). The GM80 fraction consisted of longer galactomannans less substituted in galactosyls, although these were concentrated to 83 % as substituted blocks (also grouped in “hairy” regions). The structural characterizations of GM25 and GM80 fractions have been already discussed in detail in our previous study [4].

3.2. Behavior in dilute solution

Freed from the proteins present in the starting crude LBG [4], the galactomannans viscosity of GM25 and GM80 fractions were studied. A linear plot was obtained according to the Huggins equation (Eq.3, Fig. 2) for solutions with relative viscosities (η_r) up to about 2. Extrapolation of reduced viscosity (η_{sp}/C) to zero concentration gave intrinsic viscosities of both LBG fractions: $[\eta]_{GM25} = 9.96 \text{ dL.g}^{-1}$ and $[\eta]_{GM80} = 4.04 \text{ dL.g}^{-1}$. The Kraemer plot was also carried out on a range of points for which the specific viscosity (η_{sp}) was much less than 1. The intrinsic viscosity values obtained by the Kraemer equation (Eq. 4) were $[\eta]_{GM25} = 10.3 \text{ dL.g}^{-1}$ and $[\eta]_{GM80} = 5.20 \text{ dL.g}^{-1}$. Both values were close to those obtained by Huggins equation (Eq. 3). The adjustment of the linear regression of Kraemer plot

however was not as good, due to the characteristics of these kinds of polymers. Indeed, such differences in graphical plotting for Kraemer and Huggins' extrapolations could be explained by the tendency for these compounds to aggregate with increasing concentration [18]. Huggins' values were lower than these of crude LBG found in the literature, generally between 11 and 16 dL.g⁻¹ [19, 20, 21, 22] but these crude samples also contained proteins. Other authors presented similar results to ours, on cold and hot temperature extracts of carob gum (using ethanol extraction of locust bean flour with (i) an aqueous extraction of 30 min at 25 °C (CWS) followed by a centrifugation and (ii) a re-extraction at 90 °C for 30 minutes of the centrifugation pellet previously obtained at (HWS), also punctuated with a centrifugation step) [18]. They obtained $[\eta]_{\text{CWS}}$ and $[\eta]_{\text{HWS}}$ values respectively of 8.9 dL.g⁻¹ and 6 dL.g⁻¹, also with the value for the hot extract lower than $[\eta]$ of the cold extract. The $[\eta]_{\text{GM25}}$ value is close to what was observed by Doyle et al., [6] for other galactomannans possessing a DS_{gal} closer to that of GM25 fraction, such as fenugreek gum ($[\eta]$ = 12.8 dL.g⁻¹, in water). Giannouli et al., [20] already showed that a decrease in the M/G ratio leads to an increase of the $[\eta]$ for the guar gum but this effect could be caused by some loss of galactose side chains during partial hydrolysis of native guar gum to produce grades of lower viscosity. In our case, low $[\eta]_{\text{GM80}}$ values may be attributed to decreased solute-solvent interactions. This can be confirmed by the determination of Huggins' constant. λ_{H} is a measure of polymer/polymer interaction in dilute conditions and depends upon the extent of coil expansion of the polymer coil [7]. It reflects how the viscosity of the system increases with the increase of polymer concentration, due to interaction of neighboring chains [23]. λ_{H} increases as the solvent quality decreases resulting in polymer coil contraction. Larger values possibly indicate a poorer solvent and/or polymer aggregation [7]. $\lambda_{\text{H}[\text{GM25}]}$ and $\lambda_{\text{H}[\text{GM80}]}$ were equal to 1.53 and 16.67 respectively. These values are higher than others reported (1.3 and 1.0) for crude LBG [18, 21] or other galactomannans (0.66) relatively structurally close [24] but show the same trend than a fractionated LBG, for which cold and hot extracts' λ_{H} are 0.8 and 5.1 respectively [18]. These differences in the values for LBG thus appear to be strongly related to the fractionation and/or purification process. During those processes, fractions more specific with a narrow structural distribution are selected [1], generating therefore different solvent/polymer or polymer/polymer interactions. The high values obtained for the Huggins' coefficient highlights a tendency for

association of LBG galactomannans (i.e. a poorer solubility) mainly for the GM80 extract. The lower interaction coefficient of GM25 is an indication of less intermolecular interactions in GM25 solutions. Solute/solvent interactions are greater than for GM80 but solute-solute interactions are weaker. Consequently GM25 is more soluble in water while GM80 seems to tend to self-association likely due to longer chain lengths, as previously determined. It also appears that the galactosyl distribution in GM80 induces the presence of more hydrophobic areas [4]. These structures thus favor solutions with a poor degree of dispersion containing a higher proportion of very compact aggregates which make a small contribution to the intrinsic viscosity. The intrinsic viscosity refers to the hydrodynamic volumes of the solute molecules and depends on their molecular weight [25]. The Mark-Houwink equation $[\eta] = KM^\alpha$ (Eq. 7) was used to determine molecular weights of GM25 and GM80. K and α parameters were determined by several authors. Robinson et al. (1982) thus reported $K = 0.00038$ and $\alpha = 0.723$ for galactomannans, while Picout et al., [26] obtained values of $K = 0.000296$ and $\alpha = 0.77$ for LBG. This rather simplistic model – involving only the M_w – was improved by other authors by including other structural characteristic such as DS_{Gal} [27, 28, 29]. It has also been adapted to include the specific volume [30] or the hydrodynamic volume occupied per mass unit. In this latter model, the intrinsic viscosity $[\eta]$ of disordered polymers varies with coil dimensions according to the Flory-Fox equation: $[\eta] = \Phi_F R_g^3 / M$ (Eq. 8), where R_g is the radius of gyration and Φ_F is a constant equal to $2.86 \times 10^{23} \text{ mol}^{-1}$ for random coils of linear chains [31]. These models were used to predict the expected M_w values of GM25 and GM80 fractions based on their intrinsic viscosity. The results were compared with M_w values measured by HPSEC-MALLS in our previous study [4].

Table1 :Values of GM25 and GM80 (i) based on measurements and (ii) calculated using different models proposed by other authors.

	Parameter	GM25	GM80	Type of result	Reference
Measurements	$[\eta]$ dL.g-1	10.1	4.7	Huggins equation	Present work
	X_{gal}	0.26	0.21	GC-FID	[4]
	DP_w^*	4698	5625	HP-SEC-MALLS	[4]
	PI	1.16	1.02	HP-SEC-MALLS	[4]

	$\langle Rg \rangle_w$ (nm)	91.7	106.9	HP-SEC-MALLS	[4]
	M_w (kDa)	761.1	911.3	HP-SEC-MALLS	[4]
Predicted	M_w (kDa)	1317.32	457.28	Mark Houwink model	[12]
	M_w (kDa)	769.64	284.99	Adapted Mark Houwink model	[26]
	M_w (kDa)	1561.76	667.59	Adapted Mark Houwink model	[27]
	M_w (kDa)	218.35	743.36	Floxy-Fox model	[31]

Table 1 reports the values of M_w carried out by HPSEC-MALLS on the two fractions and the M_w values calculated using different models (from $[\eta]$ and X_{gal} values). Rather important differences arise between the measurements and predictions. Such differences have also been reported on the crude LBG by Richardson et al., [7], who noted that the constants of Robinson et al., [12] lead to an overestimated value for M_w of crude LBG single chains. It seems that predictive Mark-Houwink models for galactomannans are in fact highly dependent on the technique of determination of M_w used to obtain the parameters K and α as well as the galactomannan type, the conditions of purification and/or fractionation, the sample preparation, etc. This partly explains the major differences between predictions and measurements. These models seem well adapted for crude gums but work less well on the fractions extracted from a native gum. The trend is the reverse of predicted values ($GM80 > GM25$). Moreover, unlike the fraction GM25, forecasts of GM80 fractions are always underestimated. The models seem not suitable for poorly soluble polymers. This means that in the case of fractionated extractions DS_{Gal} and M_w are probably not the only parameters to be taken into account. The distribution of side galactosyls is also suspected to play an important role on the properties and conformation of galactomannans [4]. This structural feature influences Rg . It is therefore considered in the model of Flory-Fox (Eq. 8) - not in the others - and the same trend is observed in M_w measured and determined by models, although the value for GM25 was very different. Thus, the determination of galactomannan's M_w with the Mark-Houwink equation (Eq. 7) from $[\eta]$ seems risky [21, 22, 32]. In any case, it is preferable to favor a direct measurement of M_w , especially if the results are subjected to further discussions. In a range of different disordered polysaccharides, it has been shown that $c^* \approx 4/[\eta]$, when specific viscosities $\eta_{sp} \approx 10 \cdot \eta_{sp}$ varies as $c^{1.4}$ for dilute solution and $c^{3.3}$ for semi-dilute

concentrations [12, 33]. These commonly accepted values, however, may be different from other authors' reports. Thus guar gum and LBG show a transition at lower space occupancy ($C[\eta] \approx 1.3$) and the subsequent slope was substantially steeper for semi-dilute solutions [27]. This phenomenon could be explained by the presence of more specific interactions between the molecules, in addition to non-specific physical recoveries also found for non-branched polymers. These interactions are called hyperentanglement [11] and are directly related to the fine chemical structure of galactomannans, suggesting that hyperentanglements are attributed to unsubstituted mannan sequences in the galactomannan chains [4]. From our data in Fig.3, it is not possible to determine C^* and C^{**} . Considering the slope change as corresponding to C^* , the coil overlap parameter $C[\eta]$ was determined for both fractions with $C[\eta]_{\text{GM80}}$ and $C[\eta]_{\text{GM25}}$ respectively equal to 0.931 and 1.365 for polymer concentrations respectively of 0.14 % and 0.20 %. This means that the occupancy volume of the GM25 polymers is more important. This also indicates that the GM80 chains overlap faster than GM25, although their intrinsic viscosity was lower at first (see above). The figure also indicates that η_{sp} varied depending on $(\propto) c^{1.3}$ and $c^{1.7}$ in dilute regime, for GM80 and GM25 respectively. In semi dilute regime, the tendency is the same and $\eta_{\text{spGM80}} \propto c^{3.7}$ while $\eta_{\text{spGM25}} \propto c^{2.9}$. The greater slope for GM80 fraction can be attributed to the occurrence of more polymer-polymer interactions than for GM25, again probably due to its chemical structure. Although the coil-overlap parameter is away from usually accepted values for galactomannans [33, 12] – it is in fact the case in many studies on the subject – slope values in dilute and semi-dilute regime are close to those found by other authors for LBG (Table 2). Our results may thus be compared to those reported in literature for different galactomannans or fractions of galactomannans (Table 2). When $C[\eta]$, $[\eta]$ or slopes in both regimes are plotted as a function of the M/G ratio or M_w , no correlation appears between the data. In some of the previous studies, commonly accepted values are used but not measured experimentally. Even when these last values are removed from data, no correlation appears. However, some authors have observed that a trend appears when one of these three previous parameters is plotted as a function of M/G ratio or M_w [27, 34]. It appears only for galactomannans from a specific origin and for a limited number of measurements. This suggests again that purification conditions, sample preparation and the method of measuring M_w and the M/G ratio are very important. It seems also that M_w and DS_{gal} are not sufficient

to explain the behavior of galactomannans in dilute regime. The distribution of side galactosyls seems to be an essential parameter here, as suggested by Rinaudo [35].

Table 2: Values of M_w , M/G , $[\eta]$, $C[\eta]$ and α for galactomannans found in literature.

Polymer	Reference	M_w (MDa)	Ratio M/G	$[\eta]$ (huggins)	$C[\eta]$ at C^*	α at $C < C^*$	α at $C > C^*$
disordered polysaccharides	[33]	/	/	/	4.0	1.4	3.3
Guar gum	[12]	/	/	/	4	1.3	5.1
Guar gum 1	[27]	0.38	2*	2.3	1.3	1.2	3.5
Guar gum 2	[27]	0.52	2*	2.9	1.3	1.2	3.5
Guar gum 3	[27]	0.69	2*	3.6	1.3	1.2	3.5
Guar gum 4	[27]	0.68	2*	3.8	1.3	1.2	3.5
Guar gum 5	[27]	1.2	2*	6.8	1.3	1.2	3.5
Guar gum 6	[27]	1.7	2*	10	1.3	1.2	3.5
Guar gum 7	[27]	2.02	2*	11.7	1.3	1.2	4
Locust bean gum 1	[27]	1.1	4*	7.7	1.3	1.3	3.8
Locust bean gum 2	[27]	1.33	4*	9.3	1.3	1.3	3.8
Locust bean gum 3	[27]	1.45	4*	10.1	1.3	1.3	3.8
Locust bean gum 4	[27]	1.6	4*	11.2	1.3	1.3	3.8
Locust bean gum 5	[27]	1.38	4*	10.0	1.3	1.3	3.8
<i>Mimosa scabrella</i>	[46]	/	1.1	/	2.6	1	4.2
Mesquite seed gum	[25]	/	4*	2.4	2.7	2.2	5.3
Fenugreek	[6]	/	1*	16.0	2.8	1.4	4.2
Locust bean gum	[7]	0.37	3.9	13.8	1.4	1.2	2.3
Guar gum	[7]	0.81	1.7	9.3	0.9	1.3	2.4
Guar gum	[29]	/	1.6	14.2	1.7	1.2	4.7
S egyptica	[29]	2.8	1.3	11.6	6.5	1.4	5.5
S grandiflora	[29]	2.3	1.6	8.6	3	1.5	5.1
Guar 1	[34]	2.2	/	17.2*	1.8	/	4.6
Guar 2	[34]	1.5	/	10.6*	1.9	/	4.5
Guar 3	[34]	0.3	/	4.4*	2.3	/	4
Locust bean gum	[32]	2.0*	3.3	13.5	3.3	1.2	4.8
Caesalpinia pulcherina	[32]	2.1*	2.8	13.5	3.3	1.2	4.8
Cassia javanica	[32]	1.9*	3.2	12.9	3.3	1.2	4.8
GM25 (LBG)	This work	0.76	2.85	10.1	1.3	1.3	2.9
GM80 (LBG)	This work	0.91	3.84	4.7	0.8	1.7	3.7

* Not measured. Commonly accepted values used in the work or values obtained from Eq. 7.

Thus, in dilute solutions, a higher $[\eta]$ value is generated by the GM25 fraction with more soluble galactomannans at working temperature. This kind of polymer has a larger volume occupancy and will directly increase the viscosity of a solution. Conversely, the GM80 fraction has a lower $[\eta]$ because these galactomannans are poorly soluble at room temperature and have a tendency for self-association. When the concentration increases, the less soluble galactomannans of GM80 fraction overlap faster and rapidly form hyperentanglements. Above C^* a stronger network is generated resulting in a higher apparent viscosity in semi-dilute regime. A more complete characterization of semi-dilute solutions could be obtained through rheological studies.

3.3. Behavior in unperturbed state

As demonstrated above (Fig. 3), the C^* is reached for GM25 and GM80 fractions at contents of 0.14 % and 0.20 %, respectively. This means that entanglements appear beyond these concentrations. Such

solutions can be studied with a rheometer. Fig 4 presents steady shear viscosity profiles of GM25 (blue) and GM80 (red) fractions at 0.5 %, 1 % and 2 %. These graphs demonstrate the relationship between apparent viscosity η (Pa.s) and shear rates $\dot{\gamma}$ (s^{-1}). Both fractions studied showed a shear thinning behavior for each concentration. This means that the apparent viscosity decreased as the shear rate increased. Under imposed shear stress, macromolecules are disentangled more or less quickly – depending on entanglements density and the strength of interactions – to end up oriented in the direction of the flow. This reorganization of macromolecules results in a decrease of viscosity, which is more pronounced when the concentration of the solutions increases. The apparent viscosity η on the range of shear rates tested ($\dot{\gamma}$) was greater for the fraction GM80 than GM25 at each concentration studied. η_0 and $\dot{\gamma}_{1/2}$ values, obtained from Eq. 6 are provide in Table 3. For both fractions, η_0 increased with the concentration. The increase of η_0 was also more pronounced for the GM80 fraction which reached a very high value at 2% ($\eta_{0(\text{GM80})} = 832 \text{ Pa.s}$; $\eta_{0(\text{GM25})} = 45.13 \text{ Pa.s}$). However $\eta_{0(\text{GM80})}$ at 2 % had to be obtained graphically from Fig 4. Indeed, Morris equation did not fit with the flow curve of GM80 2 % and generated an underestimated value of η_0 (172 Pa.s). $\dot{\gamma}_{1/2}$ gives a good appreciation of the shear thinning effect. Thus, for both fractions, the shear-thinning effect increased with concentration. $\dot{\gamma}_{1/2(\text{GM25})}$ showed a decrease from 93.0 to 2.2 for solutions of GM25 at 0.5 % and 2 %, respectively. This effect was however more marked for the GM80 fraction whose $\dot{\gamma}_{1/2}$ decreased from 68.6 (0.5%) to 0.3 (2%). Thus, the shear thinning effect seemed always stronger for the GM80 fraction than the GM25, for a given concentration.

Table 3: Zero-shear viscosity (η_0) and shear rate at which viscosity is reduced to $\eta_0/2$ ($\dot{\gamma}_{1/2}$) for GM25 and GM80 fraction at different concentrations in pure water at 25 °C.

Sample in water	η_0 (Pa.s)	$\dot{\gamma}_{1/2}$ (s^{-1})
GM25 0.5%	0.02	93.0
GM25 1%	3.14	12.9
GM25 2%	45.13	2.2
GM80 0.5%	0.28	68.6
GM80 1%	9.87	3.5
GM80 2%	832*	0.3

*obtained graphically from Fig 4

Analysis of Table 3 indicates that the increasing concentration resulted in an increase in the overall viscosity as well as an increase in shear-thinning behavior, as generally observed for polymers. To reveal any departures from the general form of shear thinning reported for random coil

polysaccharides, applied shear rates have been expressed as a fraction of $\gamma_{1/2}$ ($\gamma/\gamma_{1/2}$) and plotted with viscosities expressed as a fraction of η_0 (η/η_0) [16]. Fig 5 indicates that, except for GM80 2 % curve that was drawn using the η_0 obtained graphically from Fig 4, individual flow curves for both fractions converge to a single master curve – irrespective of primary structure, molecular weight and concentration – that correspond to the general form of shear thinning reported for random coil polysaccharides [33]. GM80 fraction at 2 % was a different case since it is a gel and not a solution anymore as shown in Fig 7 (Eq. 6 are applicable only for solutions). Other phenomena govern the interactions between polymers in gel state.

From steady shear profiles analyses it appears that GM80 fraction has a structure able to generate a higher viscosity in water, but paradoxically more easily able to disrupt entanglements and more easily orientable in the direction of flow (more shear-thinning). This difference in behavior between both fractions with similar structures could be explained by a greater number of hyperentanglements when the concentration in GM80 galactomannans increases. This results in the appearance of a network with many junction areas able to orient themselves in the flow direction when the shear rate increases. As previously reported, the concept of hyperentanglement can also be probed by comparison of solution properties in strong alkali and at neutral pH at the same overall ionic strength [7, 36]. Indeed, at high pH, hydroxyls groups become ionized and destabilize intermolecular associations by introducing electrostatic repulsions between the constituent chains of solutions over C^{**} . Fig 6 shows steady shear viscosity profiles for GM25 and GM80 fractions at 1 % in different media, with the same ion concentration. “NaOH” refers to a solution prepared in caustic soda, “Neut” to the soda solution neutralized with HCl, and “NaCl” to a saline solution with the same ionic strength. The steady shear viscosity profiles of 1 % galactomannan solutions in aqueous NaCl are different from those for the same measurements in water ($\eta_{0(GM25/NaCl)} = 1.9 \text{ Pa.s}$; $\gamma_{1/2(GM25/NaCl)} = 23.4 \text{ s}^{-1}$; $\eta_{0(GM80/NaCl)} = 19.7 \text{ Pa.s}$, $\gamma_{1/2(GM80/NaCl)} = 0.7 \text{ s}^{-1}$). These differences could be explained by the involvement of Na^+ and Cl^- in the network structure or by a slight difference in the concentration during solutions preparation (see below). “Neut” and “NaCl” curves contain exactly the same amount of polysaccharides (1 %) and NaCl. The obvious non-overlapping of the curves indicates that polysaccharides were partially degraded during the preparation of the “Neut” solution (3 h, 1 M NaOH, 90 °C before neutralization

with HCl). It has been reported previously that polysaccharides are susceptible to degradation under alkaline conditions, by a ‘peeling’ reaction initiated at the reducing end of the chain [37]. This seems to be the case for the two fractions studied although the impact of the degradation is less marked for GM80 fraction (perhaps due to a greater M_w). When the curves "NaOH" and "Neut" are compared with each other, major differences are observed between the two fractions. The fraction GM25 shows no significant differences between the two curves. The alkaline environment does not modify the rheology of this fraction. The GM80 fraction shows an increase in the viscosity when the solution is neutralized (curve "Neut"). This means that the alkaline medium prevents the formation of a stronger GM80 network. The rheological behavior of GM25 fraction – more substituted and with fewer smooth areas – seems essentially due to the length of the main chains and their physical recoveries. In contrast, the GM80 fraction – less substituted and with a higher number of smooth areas – shows a rheological behavior mainly influenced by alkali-labile non-covalent associations (hyperentanglements) that give rise to departure from the general behavior of concentration-dependence for disordered polysaccharides. The study of viscoelastic properties is one of the main techniques to highlight entanglements. The mechanical spectra of GM25 and GM80 fraction dispersions – at 0.5 %, 1 % and 2 % in water as well as in aqueous NaCl (1 M) – are shown in Fig 7. Except for GM80 at 2 %, graphs for dispersion in water are typical of galactomannans in semi-dilute conditions that are viscoelastic fluids generating an entangled network. The loss modulus G'' (Pa), related to the viscous component and giving the energy dissipated per cycle of deformation per unit, is greater at low oscillation frequencies than the storage modulus G' (Pa), related to the elastic component. The reverse is observed at higher frequencies. Beyond the crossover frequency (shift point), the oscillation frequency becomes too high and galactomannans chains cannot be dissociated. The interaction between the G' and G'' curves was shifted at lower frequencies for the GM80 fraction. This means that the beginning of the elastic zone ($G' > G''$) was shifted towards lower frequencies with increasing average molecular weight, M/G ratio and number of smooth areas. GM80 fractions quickly had an elastic dominance behavior generated by entanglements and hyperentanglements which dissociate less easily. For these entangled networks, the GM80 fraction has a much stronger viscoelastic behavior and greater dynamic (complex) viscosity η^* than the GM25 fraction (Fig. 4) whose G' and G'' are lower.

The case of GM80 at 2 % in water is different. The G' and G'' curves have a profile of weak gel on which no crossover is observed [38]. The elastic component G' is greater than the viscous component G'' over the entire frequency range. At this concentration, the fibers of galactomannans GM80 are thus able to “freeze” the medium by aggregation of macromolecules. They generate a three-dimensional network with a semi-solid behavior in which the solvent is trapped and cannot move freely. A 2 % content (w/v) of GM80 in pure water, heated until 90 °C, enables to reach the point of gelation. Under the same conditions, GM25 fraction does not turn into a gel, highlighting again the structural differences between the two fractions. As shown in the flow curves (Fig 6 and 7), the presence of salt in the medium can also impact the behavior, changing the mechanical spectra. The GM25 fractions in aqueous 1 M NaCl (irrespective of % w/v) exhibits viscoelastic-fluid curves almost identical to those obtained in water, with crossover frequencies similar in both media, except for GM25 fraction at 2 % that slightly shifted towards lower frequencies in H₂O. The saline environment seems to have a greater influence on GM80 fractions behavior. Indeed, GM80 fraction acts as a weak gel in all cases, even for lower concentrations in galactomannan (0.5 %). The GM80 fraction at 1 % provided the same flat spectrum as a solution of 1 % xanthan, which is considered a weak gel [39]. The GM80 mechanical spectra in aqueous NaCl (1 M) have G' and G'' curves greater by approximately a factor 10 than the same curves obtained in water. The Na⁺ and Cl⁻ ions seem interact with the polymers to “freeze” the medium and make macromolecular interactions stronger. Lyotropic effects were studied on konjac glucomannan [40] and an increase in both moduli (G' and G'') and viscosity upon addition of salting-out salts was evidenced. According to the authors, this is due to the enhancement of the salt-induced water structure perturbations or the strong interactions between ions and specific sites on the polymers. The experimental data do not permit to discuss any potential lyotropic effect here, since potential lyotropic effects of NaCl would be investigated with lyotropic series cations and anions on one GM concentration. However, NaCl is considered a relatively weak salting-out salt.

Thus, we can conclude that differences in behavior between GM25 and GM80 are simply accentuated in the presence of salt, but also with the increase in polymer concentration. Sittikijyothin et al. [11] showed mechanical spectra of CLBG in water, for which the behavior was not those of a perfect

viscoelastic fluid but trended to a weak gel. The cross point of a 1 % solution was located around 60 Hz (below 10 Hz in our case). Such differences could be explained by the fact that the measurements were performed on CLBG (still containing some proteins), without excluding that sodium azide present in the medium as a preservative could also have an influence on the galactomannans rheology. The relationship between apparent viscosity (η) and complex viscosity (η^*) can also be studied as shown in Fig. 4. Superimposability of the two viscosities – known as the Cox-Merz rule [41] is satisfied for the random coil polysaccharides in which the rheological behavior is controlled by simple physical entanglements (recovery). A difference in behavior occurred between both fractions at 2 % solutions. These phenomena are more pronounced for the GM80 fraction for which the η^* curve has a greater deviation than GM25. These observations suggest that the same types of molecular rearrangements are not occurring in both flow patterns, over the frequency range employed, i.e. a short range interaction mechanism may influence the small deformation measurement but be effectively destroyed in shear flow [42,43]. These rearrangements can be attributed to more specific associations of molecules for a larger time scale or to hyperentanglements rather than non-specific physical entanglements [33]. At 1 % and 0.5 %, η^* curves are similar and are superimposable to η curves, except for higher frequencies where they gradually diverge. Upturns in moduli and hence in η^* , at high frequencies are often seen in mechanical spectra on less concentrated solutions. They are usually attributed to the onset of resonance in the measuring geometry and were also observed on Newtonian silicone oils with similar viscosity and used as references.

3.4. Behavior in gel state

To produce solid state, the galactomannan concentration may be increased to reach gel formation, but experimentally the homogeneity of the medium is difficult to maintain. Another way is to contract viscous solutions by three freeze-thaw cycles [14]. The excess water released during the operation increases the medium concentration and generates the gel state. This operation was performed on several previously studied solutions. After three freeze-thaw cycles, solutions under 0.5 % of initial content showed visually no differences from the initial viscous solutions. Above an initial content of

0.5%, galactomannans formed a jellified pellet, more compact when the concentration increased. Three main textural parameters (hardness, cohesiveness and springiness) were extracted from the force-time curves. Results are provided in Table 4.

Table 4: Main textural parameters obtained from TPA on different galactomannan dispersion/hydrogels.

Initial solution		0%	0.05%	0.10%	0.50%	1%	2%
Hardness (N)	GM25	0.02 ± 0.00	0.03 ± 0.00	0.03 ± 0.01	0.05 ± 0.01	0.04 ± 0.01	0.11 ± 0.01
	GM80	0.02 ± 0.00	0.02 ± 0.00	0.03 ± 0.00	0.20 ± 0.03	0.47 ± 0.13	0.51 ± 0.07
cohesiveness	GM25	/	/	/	0.47 ± 0.14	0.64 ± 0.16	0.69 ± 0.03
	GM80	/	/	/	0.73 ± 0.10	0.66 ± 0.03	0.66 ± 0.06
Springiness	GM25	/	/	/	0.58 ± 0.11	0.56 ± 0.05	0.83 ± 0.02
	GM80	/	/	/	0.73 ± 0.04	0.68 ± 0.09	0.72 ± 0.03

The hardness analysis confirmed that a threshold concentration in galactomannan had to be achieved before reaching jellification. Below 0.5 % of initial galactomannan content, the hardness showed no significant difference compared with pure water. The hydrogels were formed after freeze-thaw when the initial content in the medium reached about 0.5 %. The above result simply that an interpenetration of the polymer chains is required to form such gels. Hydrogels obtained from GM80 also had a much higher hardness, suggesting again the important role of the polymer structure in the formation of the gel state. Springiness was not detectable below 0.5 % too. Above this concentration, GM80 fractions reached values of about 0.7 with no significant differences, while the 2 % GM25 fraction showed the highest value (0.83). This means that 2 % GM25 hydrogel was the most flexible and between the two compression cycles it regained a shape close to its original one. Cohesiveness is the work needed to break the internal structure of the product. This parameter makes sense only for real hydrogels. In the case of GM25, an increase in the cohesiveness was observed when the concentration increased. This implied that the most concentrated gels became stronger and less deformable. In the case of GM80, the cohesiveness at 0.5 % of initial content was higher than for GM25 fraction but it did not increase thereafter. The gels obtained with GM80 at 2 % are therefore stronger but more brittle than those obtained with GM25. Different chemical structures therefore also lead to different gel state properties through junction areas probably formed between the smooth areas of the galactomannan chains, as previously suggested in some models [44, 45]. In our case, smooth areas are more important for GM80 fraction [4] and therefore may lead to numerous junction areas. These areas could be involved in the

formation of harder and more solid gels, while a lower number of these suspected specific interactions (i.e. more "physical" entanglements) leads to the formation of softer gels (less brittle) such as those obtained with the fraction GM25. Such gels probably allow more mobility to the polymers involved in the gel network.

4. Conclusions and perspectives

This global study of viscosity demonstrates that small differences in structure within the same polymer generate different behaviors at different levels of observation (dilute solution, unperturbed state and gel state). This work also additionally highlighted that: (i) specific interactions (alkali labile non-covalent) exist between galactomannans chains – mainly for the fraction GM80 – while rheology of the GM25 fraction is more influenced by its molecular weight. According to the commonly accepted assumptions, these interactions would originate from a greater presence of non-substituted galactosyls areas on the main mannosyls chain. The regions supposedly more hydrophobic could attract themselves within the same chain in dilute regime leading to a folding which reduces the hydrodynamic volume of the polysaccharide, itself responsible for its intrinsic viscosity; (ii) the use of the Mark-Houwink equation is limited in this context; (iii) the viscoelastic behavior is modified in the presence of salt; (iv) very different gels structures are obtained according to the structure and the polymer concentrations.

In denser media, the same interactions might be the origin of hyperentanglements which form a stronger network in which each individual chain loses mobility. However at this stage, conventional tools of chemical characterization or viscosity studies did not allow the demonstration of the physical nature of such junction areas. Solid state NMR would be an interesting technique to highlight the differences in mobility within the mannosyls population of galactomannan gels, which are the expected result from specific interactions between neighbor chains.

The fundamental study of the galactomannan viscosities coupled with their structure also allows to glimpse applications that would target polymeric structures for specific properties. Thus, a fraction

such as GM25 is interesting because it imparts a viscosity at a low temperature to an aqueous medium, thus avoiding a costly and unnecessary heating in addition to a blending operation. This fraction also keeps its viscoelastic properties even in a formulation where salt content may be significant. Conversely, a fraction with low-substituted galactose as GM80 is able to give a much higher viscosity to a medium even in low concentration, which would therefore reduce the load as additive in a formulation.

Acknowledgements

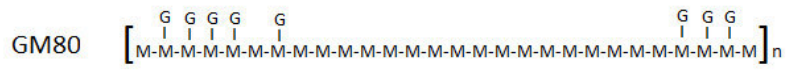
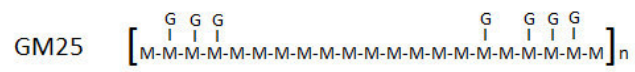
Authors thank Mrs. V. Byttebier, O. Denies and I. Van de Vreken for technical assistance.

5. References

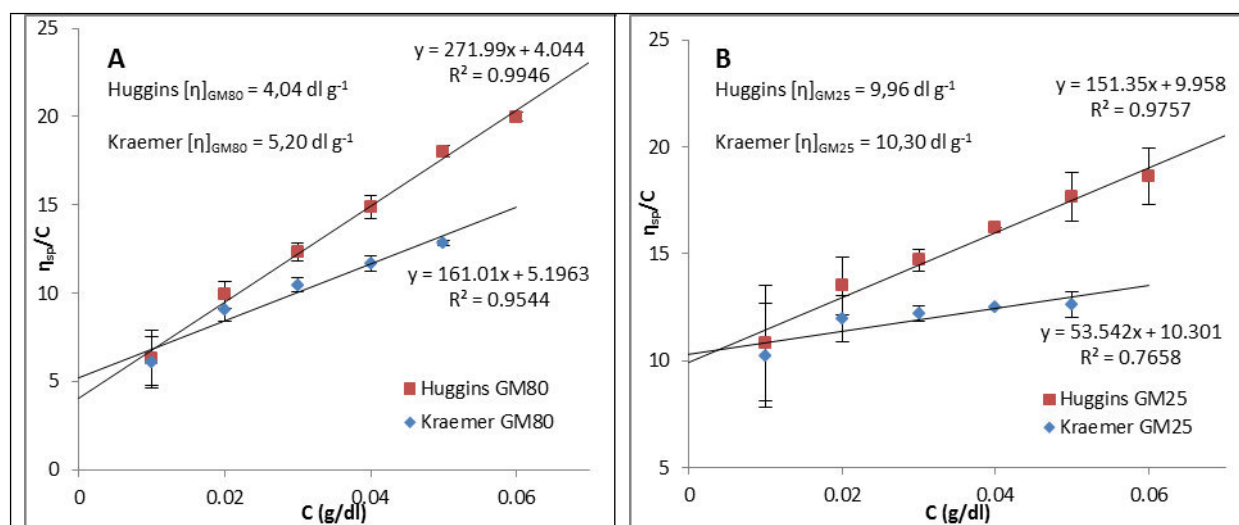
- [1] S. Gillet, C. Blecker, M. Paquot, A. Richel, Chemical structure – physical properties of galactomannans extracts from locust bean, *C. R. Chim.* 17(4) (2014) 386-401.
- [2] B. McCleary, Hydrolysis of galactomannans by α -D-galactosidase and α -D-mannanase. In J. John Marshall (Ed.), *Mechanisms of saccharide polymerization and depolymerization*, New York: Academic Press, 1980, pp. 285-300.
- [3] I. Dea, A. Morrison, Chemistry and interactions of seed galactomannans, *Adv. Carbohydr. Chem. Biochem.* 31(1975) 241-312.
- [4] S. Gillet, C. Blecker, M. Aguedo, P. Laurent, M. Paquot, A. Richel, Impact of purification and process on the chemical structure and physical properties of locust bean gum, *Carbohydr. Polym.* 108 (2014) 159-168.
- [5] S. Gillet, M. Simon, M. Paquot, A. Richel, Review of the influence of extraction and purification process on the characteristics and properties of locust bean gum, *Biotechnol. Agron. Soc. Environ.* 18 (1) (2014) 97-107.
- [6] J. Doyle, G. Lyons, E. Morris, New proposals on “hyperentanglement” of galactomannans: solution viscosity of fenugreek gum under neutral and alkaline conditions, *Food Hydrocoll.* 23 (2009) 1501-1510.
- [7] P. Richardson, J. Wilmer, T. Foster, Dilute solution properties of guar and locust bean gum in sucrose solutions, *Food Hydrocoll.* 12 (1998) 339-348.
- [8] B. Launay, G. Cuvelier, S. Martinez-Reyes, Viscosity of locust bean, guar and xanthan gum solutions in the Newtonian domain: a critical examination of the $\log (\eta_{sp})_0 - \log C[\eta]_0$ master curves, *Carbohydr. Polym.* 34 (1997) 385-395.
- [9] P.G. de Gennes, Polymer solutions in good solvents. In *Scaling concepts in polymer physics*, New York: Cornell University Press 1979, pp. 69-97.
- [10] B. Tinland, G. Maret, M. Rinaudo, Reptation in semi-dilute solutions of wormlike polymers, *Macromolecules* 23 (2) (1990), 596-602.
- [11] W. Sittikijyothin, D. Torres, M.P. Gonçalves, Modelling the rheological behavior of galactomannan aqueous solutions, *Carbohydr. Polym.* 59 (2005) 339-350.
- [12] G. Robinson, S. Ross-Murphy, E. Morris, *Carbohydr. Res.* 107 (1982), 17-32.
- [13] M. Vieira, A. Gill, A solid state NMR study of locust bean gum galactomannan and Konjacglucomannan gels, *Carbohydr. Polym.* 60 (2005) 439-448.
- [14] I. Dea, E. Morris, D. Rees, J. Welsh, H. Barnes, J. Price, Association of like and unlike polysaccharides: mechanism and specificity in galactomannans, interacting bacterial polysaccharides, and related systems, *Carbohydr. Res.* 57 (1977) 249-272.
- [15] R. Tanaka, T. Hatakeyama, H. Hatakeyama, Formation of locust bean gum hydrogels by freezeing-thawing, *Polym. Intern.* 45 (1998) 118-126.
- [16] E. R. Morris, Shear-thinning of “random coil” polysaccharides: Characterisation by two parameters from a simple linear plot, *Carbohydr. Polym.* 13 (1990) 85-96.

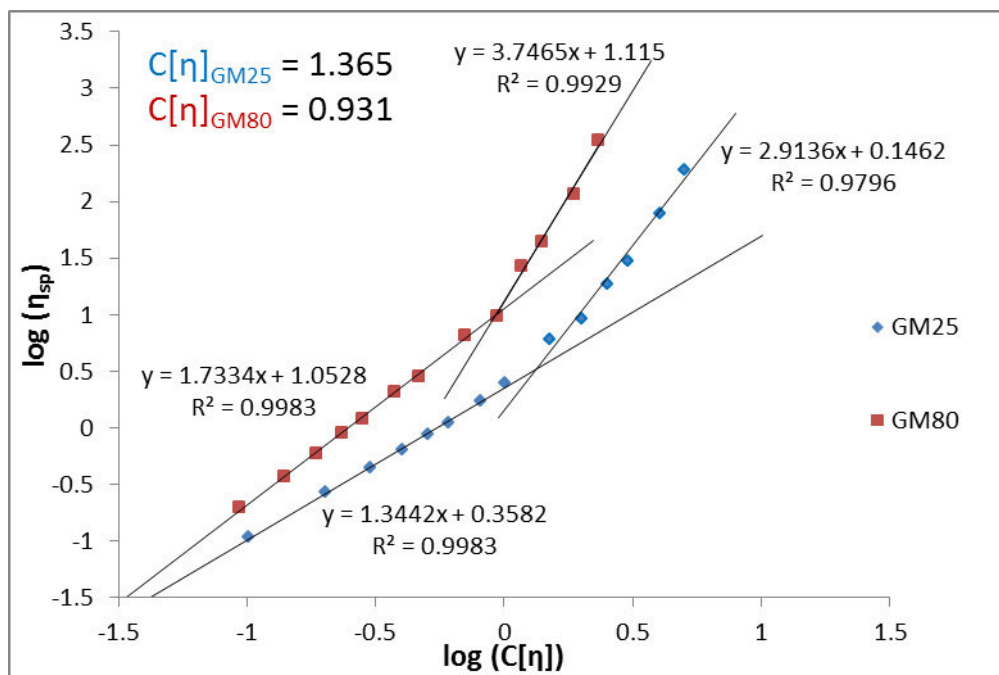
- [17] C. Blecker, M. Paquot, C. Deroanne, Gelling properties of whey proteins after enzymic fat hydrolysis, *J. Food Sci.* 65 (2000) 561-563.
- [18] S. Gaisford, S. Harding, J. Mitchell, T. Bradley, A comparison between the hot and cold water soluble fractions of two locust bean gum samples, *Carbohydr. Polym.* 6 (1986) 423-442.
- [19] E. Azero, C. Andrade, Testing procedure for galactomannan purification, *Polym. Test.* 21 (2000) 551-556.
- [20] J. Da Silva, M. Rao, Viscoelastic properties of food hydrocolloid dispersions. In: Rao, M. and Steffe, J. (Eds), *viscoelastic properties of foods*, London : Elsevier Applied Science Publishers 1992, pp. 285-315.
- [21] P. Giannouli, R. Richardson, E. Morris, Effect of polymeric cosolutes on calcium pectinate gelation. Part 1. Galactomannans in comparison with partially depolymerised starches, *Carbohydr. Polym.* 55 (2004) 343-355.
- [22] C. Mao, J. Chen, Interchain association of locust bean gum in sucrose solutions : An interpretation based on thixotropic behavior, *Food Hydrocoll.* 20 (2006) 730-739.
- [23] A. Elfak, G. Pass, G. Phillips, R. Morley, The viscosity of dilute solutions of guar gum and locust bean gum with and without added sugars, *J.Sci. Food Agric.* 28 (1977) 895-899.
- [24] R. Guo, L. Ai, N. Cao, J. Ma, Y. Wu, J. Wu, X. Sun, Physicochemical properties and structural characterization from *Sophora alopecuroides* L. seeds, *Carbohydr. Polym.* 140 (2016) 451-460.
- [25] B. Yoo, A. Figueiredo, A. Rao, Rheological properties of mesquite seed gum in steady and dynamic shear, *Lebensm.-Wis.u- Technol* 27 (1994) 151-157.
- [26] D. Picout, S. Ross-Murphy, K. Jumel, S. Harding, Pressure cell assisted solution characterization of polysaccharides. 2. locust bean gum and tara gum, *Biomacromolecules* 3 (2002) 761-767.
- [27] J. Doublier, B. Launay, Rheology of galactomannan solutions: comparative study of guar gum and locust bean gum, *J. Texture Stud.* 12 (1981) 151-172.
- [28] M. Pollard, B. Eder, P. Fisher, E. Windhab, Characterization of galactomannans isolated from legume endosperms of *Caesalpinioideae* and *Faboideae* subfamilies by multidetection aqueous SEC, *Carbohydr. Polym.* 79 (2010) 70-84.
- [29] M. Pollard, P. Fisher, E. Windhab, Characterization of galactomannans derived from legume endosperms of genus *Sesbania* (*Faboideae*), *Carbohydr. Polym.* 84 (2011) 550-559.
- [30] M. Renaud, M. Belgacem, M. Rinaudo, Rheological behaviour of polysaccharide aqueous solution, *Polym.* 46 (2005) 12348-12358.
- [31] A. Lederer, W. Burchard, A. Khalyavina, P. Linder, R. Schweins, Is the universal law valid for branched polymers? *Angew. Chem. Int. Ed.* 52 (2013) 4659-4663.
- [32] C. Andrade, E. Azero, L. Luciano, M. Goncalves, Solutions properties of the galactomannans extracted from the seeds of *Caesalpinia pulcherrima* and *Cassia javanica*: Comparison with locust bean gum, *Intern. J. Biol. Macromol.* 26 (1999) 181-185.
- [33] E. Morris, A. Cutler, S. Ross-Murphy, D. Rees, Concentration and shear rate dependence of viscosity in random coil polysaccharide solutions, *Carbohydr. Polym.* 1 (1981) 5-21.

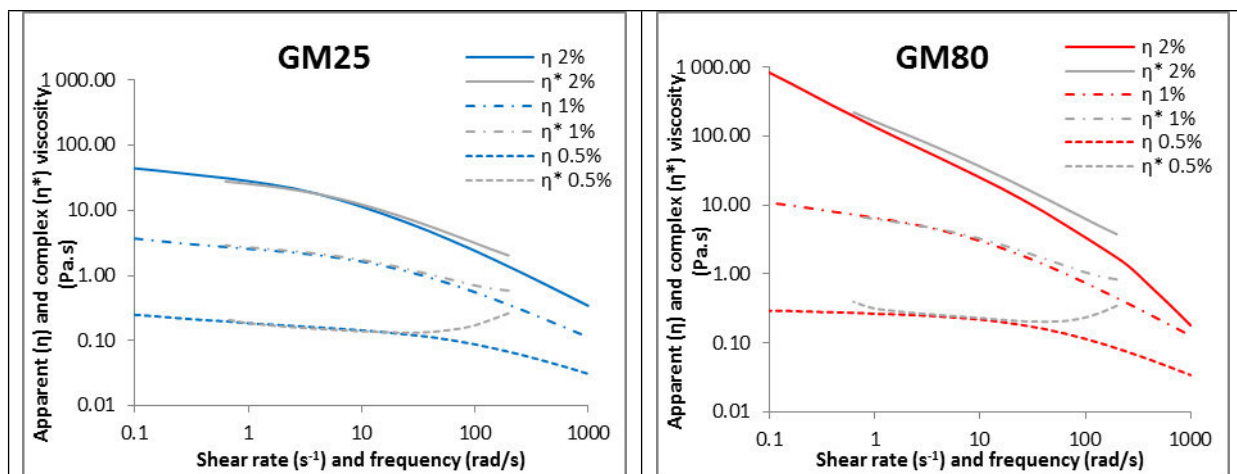
- [34] M. Pollard, P. Fischer, Semi-dilute galactomannan solutions: observations on viscosity scaling behavior of guar gum, *J. Phys.: Cond. Matter* 26 (2014) 464107.
- [35] M. Rinaudo, Relation between the molecular structure of some polysaccharides and original properties in sol and gel states, *Food Hydrocoll.* 15 (2001) 433-440.
- [36] F. Goycoolea, E. Morris, M. Gidley, Viscosity of galactomannans at alkaline and neutral pH: evidence of “hyperentanglement” in solution, *Carbohydr. Polym.* 27 (1995) 69-71.
- [37] G.O. Aspinall, *Polysaccharides*, Pergamon Press, Oxford 1970.
- [38] A. Clark, S. Ross-Murphy, Structural and mechanical properties of biopolymer gels. Biopolymers. *Advances in Polymer Science* 83, Springer Berlin, Heidelberg, 1987, pp. 57-192.
- [39] S. Ross-Murphy, Structure-property relationships in food biopolymer gels and solutions, *J. Rheol.* 39 (1995) 1451-1493.
- [40] Yin, W., Zhang, H., Huang, L., Nishinari, K., Effects of the lyotropic series salts on the gelation of konjacglucomannan in aqueous solutions, *Carbohydr. Polym.* 74 (1) (2008) 68-78.
- [41] W. Cox, E. Merz, Correlation of dynamic and steady flow viscosities, *J. Polym. Sci.* 28 (118) (1958) 619-622.
- [42] R. Richardson, S. Ross-Murphy, Non-linear viscoelasticity of polysaccharide solutions. 2: Xanthan polysaccharide solutions, *Intern. J. Biol. Macromol.* 9 (1987) 257-264.
- [43] R. Richardson, S. Ross-Murphy, Non-linear viscoelasticity of polysaccharide solutions. 1: guar galactomannan solutions, *Intern. J. Biol. Macromol.* 9 (1987) 250-256.
- [44] I. Dea, A. Clarck, B. McCleary, Effect of galactose-substitution-patterns on the interaction properties of galactomannans, *Carbohydr. Res.* 147 (1986) 275-294.
- [45] I. Dea, A. Clarck, B. McCleary, Effect of the molecular fine structure of galactomannans on their interaction properties – the role of unsubstituted sides, *Food Hydrocoll.* 1 (1986) 129-140.
- [46] J. Ganter, M. Milas, J. Corrêa, F. Reicher, M. Rinaudo, Study of solution properties of galactomannan from the seeds of *Mimosa scabrella*, *Carbohydr. Polym.* 17 (1992) 171-175.

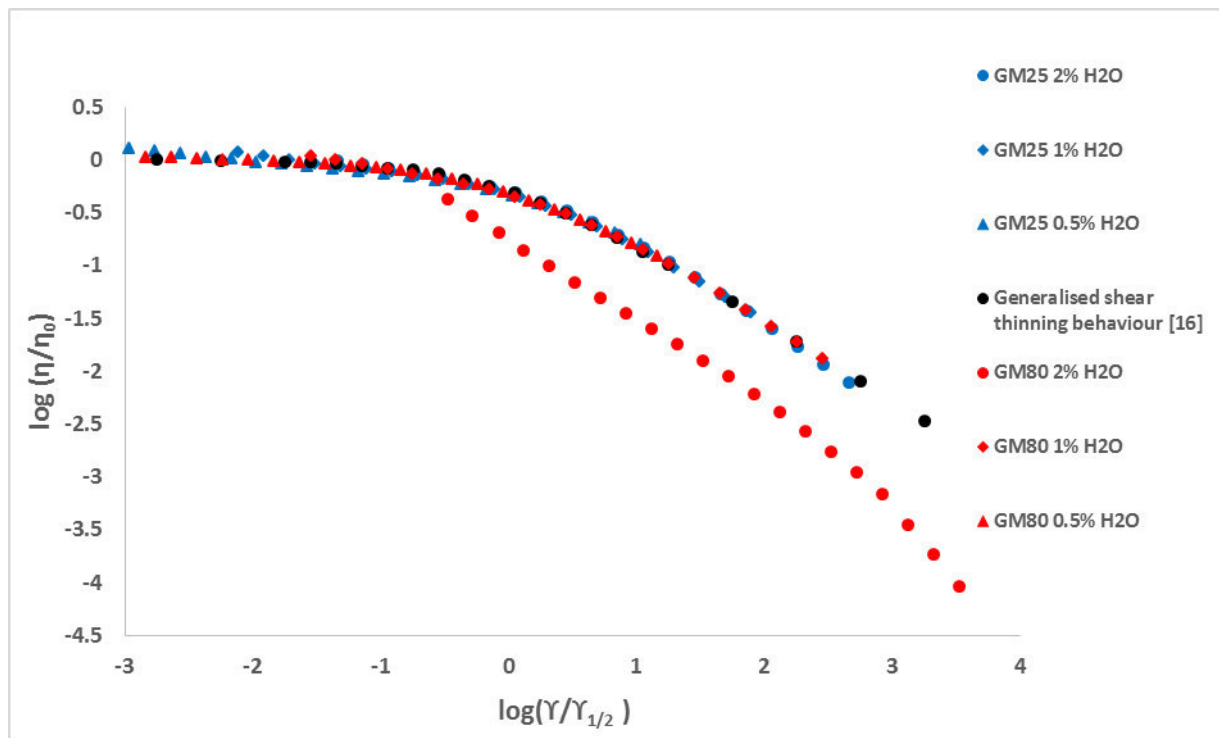


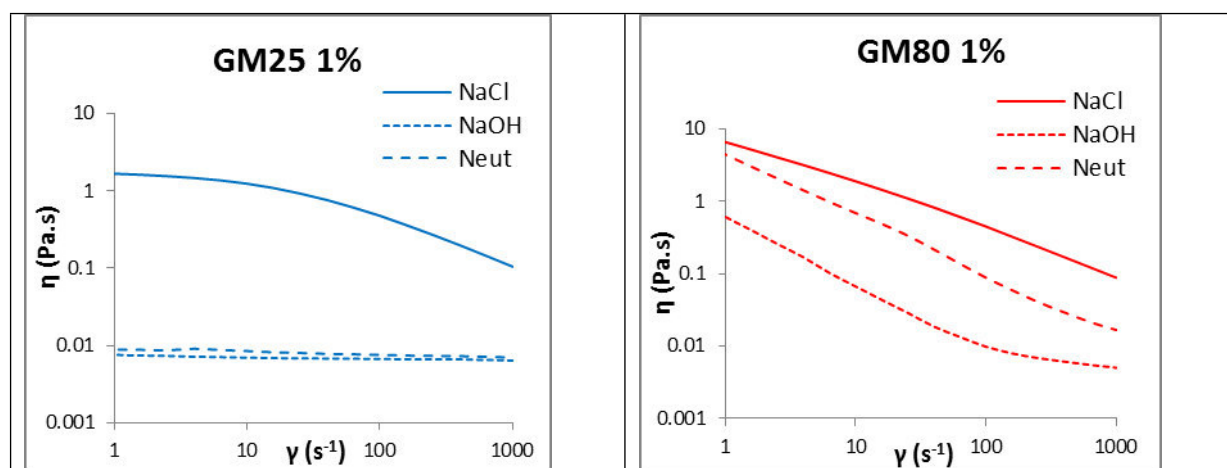
M = Mannosyl unit
G = Galactosyl unit











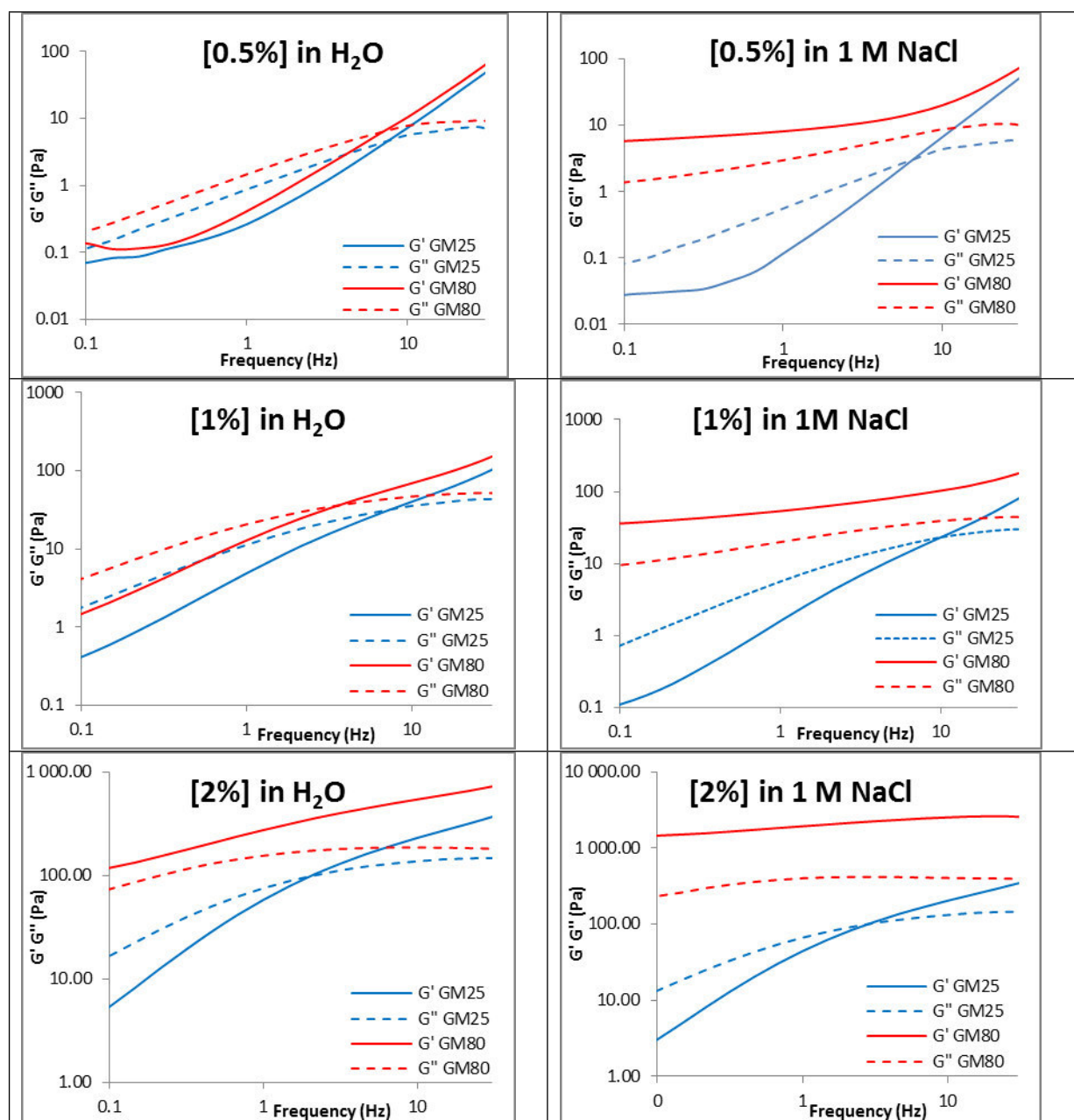


Figure 1: Schematic representation of GM25 and GM80 fractions structures. M and G are respectively mannosyl and galactosyl units. According to [4], with permission from Elsevier.

Figure 2: Huggins and Kraemer plots for GM25 and GM80 fractions in water.

Figure 3: Determination of the coil overlap parameter for both GM fractions. Standard deviations are too small to be observable on the graph.

Figure 4: Steady shear viscosity profile of GM25 (left) and GM80 (right) fractions at 0.5%, 1% and 2%.

Figure 5: Generalized shear-thinning curve for random coil polysaccharides (black spots) and comparisons to GM25 and GM80 fractions.

Figure 6: Steady shear viscosity profile of GM25 (left) and GM80 (right) fraction at 1% in alkaline medium, neutralized medium and salt water (25 °C).

Figure 7: Mechanical spectra of GM25 and GM80 fraction at different galactomannan contents in pure water (left) and salt water (right).

***Structure impact of two galactomannan fractions on their viscosity properties
in dilute solution, unperturbed state and gel state***

Abstract

Two fractions of carob galactomannans (GM25 and GM80) were extracted at respectively 25 °C and 80°C from crude locust bean gum. Those fractions having slightly different chemical structures, previously characterized, were studied for their viscosity properties over a wide range of concentrations: diluted solution, unperturbed state and gel state. For each of the physical properties, links to the chemical fine structure could be established, expanding knowledge on the topic: in dilute solution, GM25 is more soluble in water while GM80 seems to tend to self-association due to its structure as highlighted by intrinsic viscosity measurements ($[\eta]_{\text{GM25}} = 9.96 \text{ dL g}^{-1}$ and $[\eta]_{\text{GM80}} = 4.04 \text{ dL g}^{-1}$). In unperturbed state, initial viscosities η_0 were more important for GM80 fractions at 1% and 2% due to greater hyperentanglements ($\eta_{0(\text{GM80}, 1\%)} = 9.9 \text{ Pa.s}$; $\eta_{0(\text{GM80}, 2\%)} = 832.0 \text{ ; Pa.s}$ $\eta_{0(\text{GM25}, 1\%)} = 3.1 \text{ Pa.s}$; $\eta_{0(\text{GM25}, 2\%)} = 45.1 \text{ Pa.s}$). In gel state, hydrogels obtained from GM80 were also stronger (hardness GM80 (2%) = 0.51 N and hardness GM25 (2%) = 0.11 N), suggesting a much more important number of junction areas within the gel network. The findings discussed herein demonstrate the potential for new applications.